

An investigation of the annihilated unrestricted Hartree–Fock wave function and its use in secondorder Møller–Plesset perturbation theory

J. Baker

Citation: *The Journal of Chemical Physics* **91**, 1789 (1989); doi: 10.1063/1.457084

View online: <http://dx.doi.org/10.1063/1.457084>

View Table of Contents: <http://scitation.aip.org/content/aip/journal/jcp/91/3?ver=pdfcov>

Published by the AIP Publishing

Articles you may be interested in

[Explicitly correlated second-order Møller–Plesset perturbation theory for unrestricted Hartree–Fock reference functions with exact satisfaction of cusp conditions](#)

J. Chem. Phys. **131**, 084105 (2009); 10.1063/1.3212884

[Hartree–Fock and secondorder Møller–Plesset perturbation theory calculations of the \$^{31}\text{P}\$ nuclear magnetic resonance shielding tensor in \$\text{PH}_3\$](#)

J. Chem. Phys. **99**, 7819 (1993); 10.1063/1.465660

[Analytical gradients for unrestricted Hartree–Fock and second order Møller–Plesset perturbation theory with single spin annihilation](#)

J. Chem. Phys. **90**, 2363 (1989); 10.1063/1.455978

[Projected unrestricted Møller–Plesset secondorder energies](#)

J. Chem. Phys. **88**, 6991 (1988); 10.1063/1.454397

[Potential energy curves using unrestricted Møller–Plesset perturbation theory with spin annihilation](#)

J. Chem. Phys. **84**, 4530 (1986); 10.1063/1.450026



An investigation of the annihilated unrestricted Hartree–Fock wave function and its use in second-order Møller–Plesset perturbation theory

J. Baker

Department of Theoretical Chemistry, University Chemical Laboratory, Lensfield Road, Cambridge CB2 1EW, United Kingdom

(Received 29 December 1988; accepted 11 April 1989)

The recently introduced annihilated unrestricted Hartree–Fock (AUHF) wave function—in which the first spin contaminant in an unrestricted Hartree–Fock (UHF) wave function has been annihilated self-consistently—is discussed in some detail with particular attention to its use as a basis for a perturbation expansion. A series of calculations are presented highlighting the advantages and disadvantages of a second-order Møller–Plesset (AUMP2) perturbation treatment.

I. INTRODUCTION

The unrestricted Hartree–Fock (UHF) method is widely used in calculations on open shell systems. The UHF wave function generally gives reasonable spin densities, qualitatively correct dissociative behavior and, being a single determinant, forms a good basis for estimating correlation energy via Møller–Plesset perturbation theory. However, the UHF method produces wave functions that are not eigenfunctions of \hat{S}^2 and all UHF wave functions show spin contamination from higher multiplets to a greater or lesser degree.

The fact of spin contamination has been known from the early days of the UHF method but only recently has it been realized just what a problem this can be. In many cases of course, e.g., OH, NH₂ the contamination is negligible and the effects are unimportant; in others—particularly in species having multiple bonds, e.g., CN, C₂H—the problem is severe. A few examples from the literature should suffice to illustrate the extent of the problem: Pople *et al.*¹ blame spin contamination for poor UHF geometry predictions for a number of first row open shell species; Handy and co-workers² demonstrated that even “normal” radicals such as NH₂, when stretched significantly from equilibrium, develop heavily contaminated UHF wave functions which, when used as a basis for a Møller–Plesset (UMP) perturbation expansion, result in very slow convergence of the UMP series; Radom *et al.*³ similarly found that slow convergence of the UMP series due to spin contamination was responsible for poor estimates of electron affinities for a number of doublet radicals—this was confirmed in a recent study of the CN radical by Nobes *et al.*⁴

Spin contamination can be eliminated entirely at the self-consistent-field (SCF) level by using a restricted open-shell Hartree–Fock (ROHF) wave function (where the α and β MOs are constrained to have the same spatial components). However, this is not a popular approach because the ROHF wave function does not readily lend itself to subsequent use as a basis for a perturbation expansion—the formalism is much more complex for ROHF than for UHF and convergence problems are not uncommon. A similar charge can be laid against the spin extended Hartree–Fock (EHF) method. Consequently the most popular approach to reduce the contamination in UHF wave functions is spin projec-

tion⁵ using the projection operator introduced by Löwdin⁶ to annihilate higher order spin contaminants

$$\hat{P}_s = \prod_{\ell \neq s} \frac{\hat{S}^2 - \ell(\ell + 1)}{S(S + 1) - \ell(\ell + 1)}. \quad (1)$$

In most cases, the major contaminant in an UHF wave function comes from the next highest spin multiplicity, and typically only this, and possibly the next contaminant, are eliminated. It does not seem feasible to use the full projection operator (1) in actual calculations.

Results obtained with the projected UHF (PUHF) wave function are not particularly impressive in themselves; the value of spin projection is that it can be applied at the correlated level to UMP wave functions. This has recently been done by Schlegel⁷ who developed an approximate formalism to project out the first contaminant at the UMP2, UMP3, and UMP4 levels, and Knowles and Handy⁸ who used a more consistent formalism to remove the first two contaminants from UMP2 wave functions. Both authors have presented results showing considerable improvements over unprojected wave functions.

The purpose of this paper is to present details of a new wave function—the annihilated unrestricted Hartree–Fock (AUHF)⁹—which is a UHF wave function in which the first spin contaminant has been annihilated self-consistently. The usefulness of the AUHF wave function as a basis for perturbation calculations has already been demonstrated for a number of doublet radicals.¹⁰ In this work the method is described more fully and a series of calculations reported on the geometries of a number of first row systems, the electron affinities of several doublet radicals, the barrier for the addition of hydrogen to ethylene and the dissociation of the CN radical.

II. THE AUHF METHOD

The precise sequence of steps taken in the AUHF procedure is shown in Fig. 1. Basically the same steps as in a normal UHF calculation are followed except that the first spin contaminant is annihilated from the density matrix before constructing the Fock matrix. Convergence can be on either the projected ρ^* or unprojected density ρ (the final results are the same) and in this sense the procedure is self-consistent. In Ref. 10 it was (mistakenly) stated that *all* of

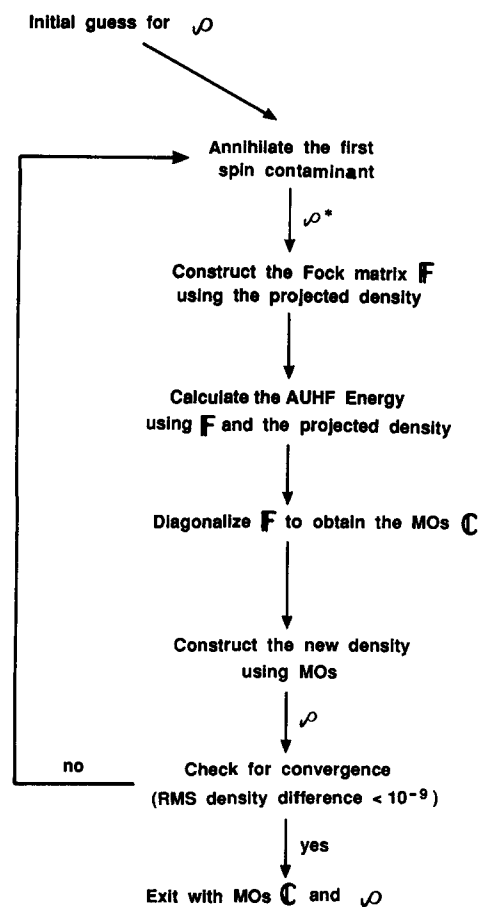


FIG. 1. Schematic of the AUHF procedure.

the first contaminant was removed from the final AUHF wave function; this is not the case (since the final wave function C is derived from ρ and not ρ^*) and, in fact, most of what little contamination does remain comes from the next highest spin multiplicity—contamination from higher order multiplets is almost zero. It is also clear that—in contrast to the speculation in Ref. 10—the AUHF and ROHF methods are not equivalent even if the full projection operator in Eq. (1) were used, i.e., even if *all* spin contamination were removed from the wave function. This can be seen from calculations on the lithium atom for which a single projection is sufficient to remove all the contamination: UHF, AUHF, and ROHF energies are different. In fact, it would be very surprising if the α and β MOs were to become identical given that there are more α electrons than β for any open-shell system and so the Fock operators are different for each spin.

The AUHF method is extremely efficient in removing spin contamination. In all cases examined so far residual contamination is under 2%. For example, $\langle \hat{S}^2 \rangle$ for CN with the STO-3G basis is reduced from 1.2283 to 0.7570; similarly $\langle \hat{S}^2 \rangle$ for BO falls from 0.9178 to 0.7556.¹⁰

As well as the remarkable reduction in spin contamination the AUHF method has a number of distinct advantages over PUHF. If we look first at MP perturbation theory, because any contamination in the underlying UHF wave function persists throughout the perturbation series, spin projection as in Refs. 7 and 8 has to be carried out order by order. This becomes increasingly more difficult at higher orders. The AUHF wave function, on the other hand, is capable of forming the basis for a perturbation expansion in its own

TABLE I. Optimized equilibrium geometries with the 6-31G* basis set. (Bond lengths in Å; bond angles in degrees.)

Species	Parameter	Expt.	ROHF	UHF	$\langle S^{*2} \rangle$	AUHF	$\langle S^{*2} \rangle$	UMP2	AUMP2
BeH	$r(\text{BeH})$	1.343	1.346	1.348	0.752	1.346	0.7505	1.348	1.346
BH ₂	$r(\text{BH})$	1.181	1.186	1.185	0.752	1.186	0.7510	1.188	1.189
	$\angle \text{HBH}$	131	126.2	126.5		126.2		127.6	127.3
OH	$r(\text{OH})$	0.970	0.958	0.959	0.755	0.958	0.7524	0.979	0.979
CH	$r(\text{CH})$	1.120	1.107	1.108	0.756	1.107	0.7529	1.120	1.120
NH ₂	$r(\text{NH})$	1.024	1.012	1.013	0.758	1.012	0.7532	1.029	1.028
	$\angle \text{HNNH}$	103.3	104.3	104.4		104.3		103.3	103.3
CF	$r(\text{CF})$	1.272	1.267	1.267	0.759	1.267	0.7538	1.291	1.289
CH ₃ ^a	$r(\text{CH})$	1.079	1.071	1.073	0.761	1.071	0.7539	1.079	1.078
NO ₂	$r(\text{NO})$	1.197	1.162	1.165	0.767	1.162	0.7568	1.216	1.216
	$\angle \text{ONO}$	134.3	136.5	136.1		136.5		133.7	133.6
BO	$r(\text{BO})$	1.205	1.185	1.187	0.800	1.185	0.7535	1.217	1.221
OCN	$r(\text{CN})$	1.23	1.230	1.213	0.835	1.229	0.7568	1.253	1.251
	$r(\text{OC})$	1.18	1.142	1.160		1.142		1.166	1.184
CN	$r(\text{CN})$	1.175	1.137	1.162	1.127	1.138	0.7573	1.135	1.202
C ₂ H	$r(\text{CC})$	1.207	1.185	1.215	1.165	1.185	0.7580	1.180	1.219
	$r(\text{CH})$	1.061	1.057	1.058		1.057		1.065	1.066
NH	$r(\text{NH})$	1.036	1.021	1.024	2.014	1.021	2.0068	1.040	1.038
CH ₂	$r(\text{CH})$	1.078	1.072	1.071	2.015	1.071	2.0059	1.077	1.078
	$\angle \text{HCH}$	136	128.4	130.4		128.9		131.6	129.9
NF	$r(\text{NF})$	1.317	1.305	1.302	2.019	1.303	2.0098	1.330	1.331
O ₂	$r(\text{OO})$	1.208	1.163	1.168	2.032	1.164	2.0182	1.242	1.248
HNC	$r(\text{NH})$		1.013	1.017	2.347	1.014	2.0140	1.036	1.037
	$r(\text{CN})$		1.236	1.271		1.237		1.229	1.270
	$\angle \text{HNC}$		112.6	111.5		112.9		113.5	111.7
LiCl ^b	$r(\text{LiCl})$		1.956	2.037	2.805	1.962	2.0083	2.013	1.970

^a Planar; D_{3h} .^b Linear.

right, and since it is virtually free of contamination no further projection needs to be done. In addition, despite the fact that the Fock matrix is constructed using the *projected* density while the MOs are derived from the *unprojected* density, numerical tests show that—provided the initial contamination is not excessive (i.e., ρ^* does not differ excessively from ρ)—analytical gradients can be obtained in precisely the same way as for a normal UHF wave function *using the same code*. This also applies to AUMP2 gradients, although not to the same extent. This is not as good as it sounds since,

in practice, as the initial spin contamination increases geometries obtained analytically become less reliable and it is precisely the highly contaminated systems for which the method is the most useful. However the results are still surprisingly good: For example, the difference in the final AUHF geometries for the species shown in Table I optimized analytically (using analytical gradients) and numerically (estimating the gradient by finite difference on the energy) is virtually nil for the low to moderately contaminated systems rising to $\sim 0.001 \text{ \AA}$ (10^{-6} hartree in the energy) for

TABLE II. (A) Energies of selected doublet species from Table I, 6-31++G** basis set. (B) 6-311++G** basis set.

Species	UMP2	UMP3	UMP4	AUMP2	AUMP3	AUMP4
(A) OH	-75.541 23	-75.552 68	-75.557 16	-75.538 48	-75.549 96	-75.554 46
Anion	-75.602 58	-75.595 84	-75.611 31			
NH ₂	-55.716 13	-55.731 56	-55.736 31	-55.713 31	-55.728 78	-55.733 54
Anion	-55.731 48	-55.734 48	-55.746 82			
NO ₂	-204.574 58	-204.545 93	-204.604 08	-204.571 44	-204.540 70	-204.600 89
Anion	-204.648 23	-204.625 88	-204.677 37			
BO	-99.763 33	-99.756 31	-99.777 70	-99.763 26	-99.755 03	-99.778 20
Anion	-99.843 04	-99.839 37	-99.862 85			
OCN	-167.553 79	-167.557 43	-167.589 25	-167.555 01	-167.553 46	-167.589 45
Anion	-167.693 68	-167.678 76	-167.719 25			
CN	-92.440 04	-92.446 39	-92.467 34	-92.465 21	-92.455 83	-92.488 43
Anion	-92.603 40	-92.598 98	-92.624 71			
C ₂ H	-76.357 56	-76.372 03	-76.386 92	-76.370 88	-76.380 16	-76.397 37
Anion	-76.474 56	-76.479 85	-76.501 74			
(B) OH	-75.579 81	-75.590 14	-75.595 53	-75.577 10	-75.587 44	-75.592 86
Anion	-75.640 01	-75.630 64	-75.650 01			
NH ₂	-55.737 53	-55.752 32	-55.758 08	-55.734 73	-55.749 54	-55.755 32
Anion	-55.755 44	-55.757 02	-55.771 85			
NO ₂	-204.667 31	-204.633 52	-204.701 01	-204.664 16	-204.628 21	-204.697 95
Anion	-204.736 31	-204.709 37	-204.769 20			
BO	-99.805 31	-99.796 00	-99.821 08	-99.805 24	-99.794 62	-99.821 56
Anion	-99.886 71	-99.881 32	-99.908 82			
OCN	-167.622 41	-167.623 01	-167.659 38	-167.622 93	-167.618 00	-167.658 98
Anion	-167.760 75	-167.741 88	-167.788 60			
CN	-92.469 42	-92.474 51	-92.497 78	-92.493 08	-92.481 91	-92.517 95
Anion	-92.634 06	-92.628 14	-92.657 11			
C ₂ H	-76.380 49	-76.394 80	-76.410 98	-76.393 34	-76.402 27	-76.421 06
Anion	-76.500 07	-76.505 39	-76.528 61			

the C-N and C-C bond lengths in CN and C₂H. The AUMP2 results are not as good and although errors are again essentially nil for all the doublets up to and including OCN, the error in the C-C bondlength in C₂H is 0.009 Å (2×10^{-4} hartree). Even though this latter result is unacceptable, a simple remedy in suspect cases is to reoptimize the geometry numerically starting from the final analytical geometry. Convergence should be very rapid.

Although it clearly has many advantages the AUHF method does suffer from the disadvantage that it cannot be used for open shell singlets. Attempts to use it in such situations invariably result in convergence to the RHF solution.¹⁰ For singlets, therefore, PUMP2 schemes must still be used.

Results obtained at the AUHF level are similar to those obtained using the ROHF method. This has already been demonstrated for energies in Ref. 10 and can be seen for equilibrium geometries in Table I; optimized AUHF and ROHF geometries for all systems examined are virtually the same. Thus, as far as equilibrium properties are concerned AUHF shows no advantages over ROHF and if ROHF gradients are available this should be the method of choice. As with the PUHF method, AUHF comes into its own at correlated levels, especially AUMP2 for which analytical gradients are readily available, as discussed above.

III. AUMP PERTURBATION THEORY

The effects of the AUHF wave function on the energies and rate of convergence of the Møller-Plesset perturbation series has already been shown.¹⁰ This section concentrates mainly on the AUMP2 wave function and its utility for geometry and energy predictions in *ab initio* calculations.

A. Geometries

Table I gives the optimized equilibrium geometries for a selection of first row radicals using the 6-31G* basis¹¹ at the ROHF, UHF, AUHF, UMP2, and AUMP2 levels of theory. The radicals chosen were mostly taken from table 6.22 of Ref. 1 with a number of additions and deletions and in many

cases the ROHF, UHF, and UMP2 geometries were taken directly from this table. All calculations were done with a modified version¹² of GAUSSIAN 82.¹³ For the more contaminated species geometries obtained analytically were refined numerically as outlined in the previous section.

Doublet and triplet species are listed separately and tabulated in order of increasing spin contamination in the UHF wave function. The efficacy of the AUHF method in reducing spin contamination is clear from the table. The general trend as far as geometries are concerned¹ is that bond lengths calculated at the SCF level are too short whereas those at the MP2 level are too long, although usually showing better agreement with experiment. This trend is clearly observed in the majority of systems having low spin contamination for which in all cases (except BeH) the bond length increases on going from UHF to UMP2. However, for the species showing the highest spin contamination, CN and C₂H (doublets) and HNC and LiCl (triplets), the UMP2 bondlengths actually decrease. That this is due to spin contamination can be seen from the AUMP2 results where all bond lengths increase (again except BeH) relative to AUHF, including those for C₂H, CN, HNC, and LiCl.

B. Electron affinities

Table II gives the MP2, MP3, and MP4 energies of those doublets in Table I for which reliable electron affinities are known experimentally; the corresponding theoretical EAs (obtained by energy difference from the anion) are shown in Table III. Calculations were carried out with the 6-31++G** and 6-311++G** basis sets using the optimized geometries (UMP2 and AUMP2 as appropriate) given in Table I; for the anions optimized RMP2/6-31G* geometries were used.

Comments on the convergence pattern of the MP energies have already been made in Ref. 10; suffice it to say that convergence of the AUMP series is similar to that of the RMP series (c.f., the anions). As far as the magnitudes of the MP energies are concerned, for doublet species with low

TABLE III. (A) Electron affinities (eV) of doublet species from Table I, 6-31++G** basis set. (B) 6-311++G** basis set.

Species	Expt.	UMP2	UMP3	UMP4	AUMP2	AUMP3	AUMP4
(A) OH	1.83 ± 0.01	1.67	1.17	1.47	1.74	1.25	1.55
NH ₂	0.78 ± 0.04	0.42	0.08	0.29	0.49	0.16	0.36
NO ₂	2.32 ± 0.04	2.00	2.18	1.99	2.09	2.32	2.08
BO	3.1 ± 0.1	2.17	2.26	2.32	2.17	2.29	2.30
OCN	3.6 ± 0.2	3.81	3.30	3.54	3.77	3.41	3.53
CN	3.82 ± 0.02	4.45	4.15	4.28	3.76	3.90	3.71
C ₂ H	2.94 ± 0.10	3.18	2.93	3.12	2.82	2.71	2.84
(B) OH	1.83 ± 0.01	1.64	1.10	1.48	1.71	1.18	1.56
NH ₂	0.78 ± 0.04	0.49	0.13	0.37	0.56	0.20	0.45
NO ₂	2.32 ± 0.04	1.88	2.06	1.86	1.96	2.21	1.94
BO	3.1 ± 0.1	2.21	2.32	2.39	2.22	2.36	2.37
OCN	3.6 ± 0.2	3.76	3.23	3.52	3.75	3.37	3.53
CN	3.82 ± 0.02	4.48	4.18	4.34	3.84	3.98	3.79
C ₂ H	2.94 ± 0.10	3.25	3.01	3.20	2.90	2.81	2.93

TABLE IV. Barrier heights for the addition of hydrogen to ethylene (kcal mol⁻¹).

Method ^a	UHF/6-31G* geometries		UMP2/6-31G* geometries	
	6-31G*	6-311++G**(6D) ^b	6-31G*	6-311++G**(6D) ^b
UHF	2.90	3.70		
UMP2	11.87	10.49	12.90	10.40
PUMP2 ^c	4.02 (−1.84)	3.11	4.69	2.57
PUMP2 (2) ^d	3.24	2.30	4.13	1.92
AUMP2	7.15	6.13	11.13	8.69
Expt.	2.04 ± 0.08			

^a All orbitals are included in the correlation treatment.^b Six Cartesian d orbitals used with the 6-311++G** basis.^c Schlegel method (Ref. 7).^d Knowles and Handy method (Ref. 8).

spin contamination (<0.8), AUMP energies are higher than UMP; for intermediate spin contamination (0.8–0.9) AUMP and UMP energies are similar, while for high spin contamination (>0.9) AUMP energies are lower than UMP. Since the general trend is for calculated electron affinities of low spin contaminated systems to be too low and high spin contaminated to be too high, AUMP EAs should show as good as or better agreement with experiment than UMP across the board. That this is indeed the case can be clearly seen from Table III; AUMP EAs are better than UMP at all orders for virtually all species. These results confirm the tentative conclusions given in Ref. 10 as to the usefulness of the AUMP approach for calculating electron affinities and further highlight the suitability of AUMP2 in particular in this regard.

C. The addition of hydrogen to ethylene

The effect of spin contamination on the barrier height for this process has recently been investigated by Sosa and Schlegel¹⁴ and Knowles and Handy.⁸ They both carried out single point UMP and PUMP energy calculations with the 6-31G* basis on minimum and transition state geometries optimized at the SCF level. Their results are summarized in Table IV along with those from a similar AUMP calculation and additional calculations using UMP2/6-31G* optimized geometries and a larger (6-311++G**) basis set. The geometries of the two species are given in Fig. 2.

As is clear from the table, removing the spin contamination reduces the calculated MP2 barrier in all cases, although the AUMP2 values are not as good as with the two projection schemes.^{8,14} $\langle \hat{S}^2 \rangle$ at the transition state is of the order of 0.97 and at this level of contamination, AUMP energies are only slightly lower than UMP. It would appear that the *worse* the spin contamination the *more* there is to be gained by using the AUMP wave function, i.e., the *greater* the energy difference between E_{UMP2} and E_{AUMP2} .

Note that in Sosa and Schlegel's original work,¹⁴ their quoted PUMP2/6-31G* barrier is -1.84 kcal mol⁻¹ (given in parentheses in Table IV); this value is also quoted in Table IV of Ref. 8. However, Schlegel's barrier was calculated using frozen core whereas Knowles and Handy included *all* orbitals in the correlation treatment (as is also the case in

this work). The quite dramatic change in barrier height (-1.84 to 4.02 kcal mol⁻¹) when the core orbitals are included indicates that these orbitals play a significant role as far as spin contamination is concerned.

Since AUMP2 gradients can be obtained at no extra

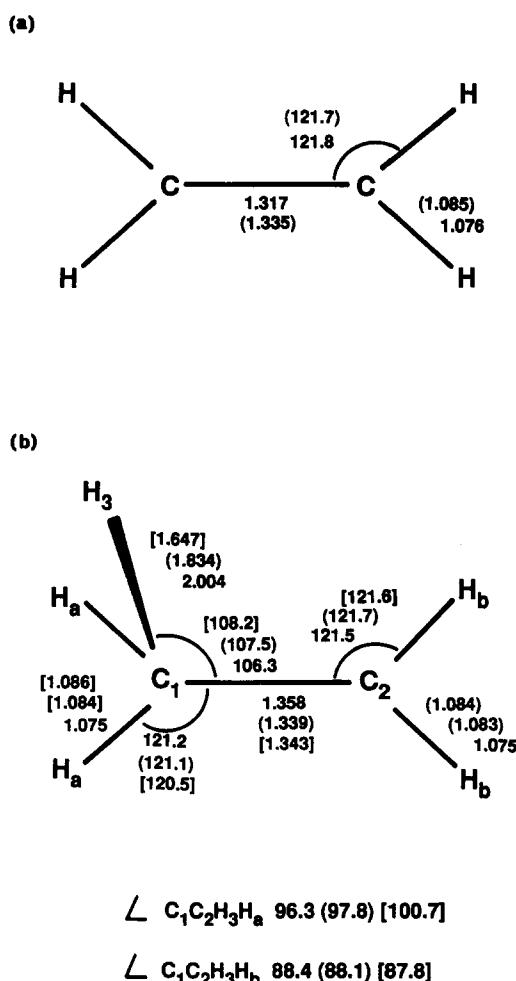


FIG. 2. Geometry of (a) C₂H₄ and (b) C₂H₅ with the 6-31G* basis set (bond lengths in Å; bond angles in degrees). () UMP2; [] AUMP2; other values UHF.

TABLE V. Calculated energies of CN at various levels of theory with the STO-3G basis set from 1.0–1.7 Å.

Å	UHF	UMP2	PUMP2	PUMP2(2)	ROHF	AUHF	AUMP2	Full CI
1.0	–90.895 37	–90.992 98	–90.999 53	–91.000 59	–90.888 56	–90.888 85	–90.993 79	–91.016 43
1.1	–90.996 78	–91.102 02	–91.119 49	–91.122 79	–90.983 98	–90.984 29	–91.117 61	–91.139 11
1.2	–91.024 99	–91.110 55	–91.151 30	–91.153 14	–90.994 33	–90.994 74	–91.162 54	–91.178 45
1.3	–91.022 51	–91.085 49	–91.142 74	–91.133 92	–90.958 93	–90.959 62	–91.166 35	–91.172 33
1.4	–91.006 30	–91.055 02	–91.115 12	–91.096 26	–90.903 18	–90.904 60	–91.139 19	–91.143 29
1.5	–90.983 05	–91.023 92	–91.077 48	–91.054 40	–90.841 70	–90.843 29	–91.096 91	–91.104 55
1.6	–90.955 83	–90.992 92	–91.035 64	–91.013 52	–90.777 95	–90.779 49	–91.058 58	–91.063 69
1.7	–90.926 30	–90.962 29	–90.993 35	–90.975 08	–90.715 44	–90.716 87	–91.022 51	–91.025 04

effort using standard UMP2 code, it is of interest to optimize the ethylene–hydrogen transition state and calculate a genuine AUMP2/6-31G* barrier. The geometry of the AUMP2 TS thus obtained (refined numerically as discussed in Sec. II) is given in Fig. 2 and it can be seen that the long C–H distance decreases significantly compared to both the UHF and UMP2 distances (2.004, 1.834, and 1.647 Å, respectively). The calculated barrier height of 14.79 kcal mol^{–1} is much worse than barriers calculated using the SCF or UMP2 geometries. This is perhaps not too surprising when it is borne in mind that the underlying AUHF wave function—which can be considered as more or less equivalent to ROHF—is unsuitable for describing dissociation processes; thus despite the spin contamination, the UMP2 geometry is likely to be more reliable than the AUMP2. This can be seen more clearly in the next example.

D. Dissociation of the CN radical

Calculated energies at the UHF, UMP2, PUMP2,⁷ PUMP2(2),⁸ ROHF, AUHF, AUMP2, and full configuration interaction (CI) levels for the CN radical with the STO-3G basis set are given in Table V for C–N distances between 1.0 and 1.7 Å; corresponding dissociation curves are shown in Fig. 3. All orbitals were included in the correlation treatment.¹⁵

CN is highly spin contaminated and in this case the AUMP2 potential energy curve shows the best agreement with the full CI results. Note that as the C–N distance increases, the energies for both the projected UMP2 schemes tends towards the UMP2 energy (at large distances—not shown—this is very marked). $\langle S^2 \rangle$ increases with increasing C–N distance and the AUHF wave function is more capable

of coping with the increasing spin contamination as evidenced by Table VI, which shows $\langle S^2 \rangle$ values for the UHF, AUHF, and PUMP2(2) wave functions.

For CN the AUMP2 method cannot be pushed beyond a C–N distance of about 1.7 Å. This is because the underlying ground state AUHF wave function switches, i.e., the state “followed” between 1.0–1.7 Å is no longer the lowest energy state at larger C–N distances and the perturbation treatment breaks down. The same thing happens for UMP2, but at much larger distances. Convergence difficulties for the AUHF wave function are also encountered at this point.

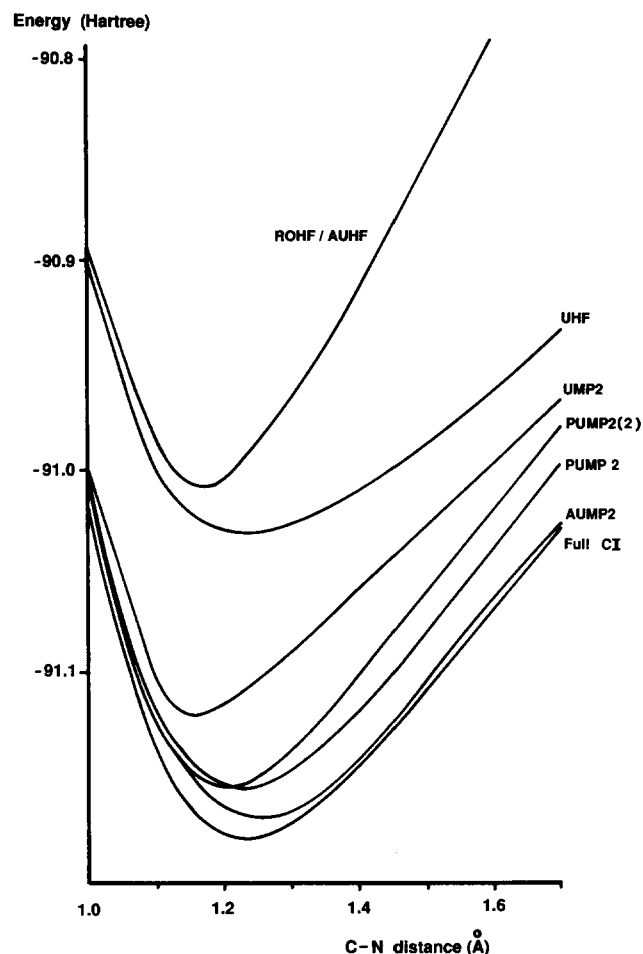


FIG. 3. Potential energy curves for the dissociation of CN from 1.0 to 1.7 Å at various levels of theory with the STO-3G basis set (from the energies given in Table V).

TABLE VI. $\langle S^2 \rangle$ for CN for the UHF, AUHF, and PUMP2(2) wave functions (see Table V).

Å	UHF	PUMP2(2)	AUHF
1.0	0.8204	0.7500	0.7550
1.1	0.9870	0.7500	0.7562
1.2	1.4044	0.7507	0.7575
1.3	1.8312	0.7544	0.7586
1.4	2.1459	0.7626	0.7603
1.5	2.3613	0.7743	0.7617
1.6	2.5061	0.7884	0.7625
1.7	2.6029	0.8040	0.7622

This illustrates a weakness in the AUMP2 method—based as it is on the AUHF wave function—in that, it cannot handle dissociation properly. This was alluded to in the previous section. In order for a single determinant-based wave function to dissociate properly it must be extremely flexible, and the UHF wave function which is much less constrained than the AUHF is better able to cope in this regard, as can be clearly seen from the dissociation curves in Fig. 3. Examination of the full CI wave function shows that at 1.7 Å no one determinant dominates; instead there are about a dozen determinants with a weighting of greater than 0.1 and no single determinant has a chance of coping in this region.

IV. CONCLUSIONS

The AUHF method represents an efficient, easily implemented procedure for virtually eliminating spin contamination in high spin (doublets or greater) UHF wave functions. It gives energies very close to those for the corresponding ROHF wave function and, as far as perturbation theory is concerned, can be thought of as a way of doing Møller-Plesset ROHF perturbation calculations without actually using an ROHF wave function. It shows a number of advantages in this regard:

(1) Unlike the various projection schemes, the AUHF wave function itself can be used as the basis for a perturbation expansion; there is no need for an order-by-order projection.

(2) Analytical gradients, second derivatives and other properties are available in exactly the same way as for a normal UMP wave function (although caution is required for highly contaminated systems).

However, there are also a number of disadvantages.

(1) Although spin contamination will be reduced there is no guarantee that the resulting AUMP energy will be lower than the UMP energy. The method appears to work best the greater the initial contamination—there is a cutoff ($\langle \hat{S}^2 \rangle \approx 0.8$ for doublets) beyond which the AUMP energy will be reduced but below which it will not. Thus, the method is not uniformly applicable.

(2) Because of the inability of the underlying AUHF

wave function to adequately describe dissociation, the AUMP2 method can only really be used in the region of the minimum. It should be used with considerable caution when attempting to describe transition structures.

Both the above are likely to be weaknesses of an ROHF, as well as AUHF, wave function. Thus, if ROHF perturbation theory were done properly the same comments would apply.

The AUMP2 method represents another weapon in the quantum chemists armoury, to be used where appropriate depending on the circumstances. As with all other wave functions it has advantages and disadvantages. Hopefully these have been clarified in this paper. As an efficient method for calculating reliable electron affinities it can be strongly recommended.

ACKNOWLEDGMENTS

Valuable discussions with Dr. N. C. Handy are gratefully acknowledged. Many of the calculations were done on the Organic Chemistry microVAX at Imperial College, London and thanks are due to Dr. H. Rzepa for the generous allocation of CPU time.

¹W. J. Hehre, L. Radom, P. v. R. Schleyer, and J. A. Pople, *Ab Initio Molecular Orbital Theory* (Wiley, New York, 1986).

²N. C. Handy, P. J. Knowles, and K. Somasundram, *Theor. Chim. Acta.* **68**, 87 (1985).

³J. Baker, R. H. Nobes, and L. Radom, *J. Comp. Chem.* **7**, 349 (1986).

⁴R. H. Nobes, J. A. Pople, L. Radom, N. C. Handy, and P. J. Knowles, *Chem. Phys. Lett.* **138**, 481 (1987).

⁵A. T. Amos and G. G. Hall, *Proc. R. Soc. London* **263**, 483 (1961).

⁶P. O. Löwdin, *Phys. Rev.* **97**, 1509 (1955).

⁷H. B. Schlegel, *J. Chem. Phys.* **84**, 4530 (1986).

⁸P. J. Knowles and N. C. Handy, *J. Chem. Phys.* **88**, 6991 (1988).

⁹T. Kovar (private communication).

¹⁰J. Baker, *Chem. Phys. Lett.* **152**, 227 (1988).

¹¹(a) P. C. Hariharan and J. A. Pople, *Theor. Chim. Acta.* **28**, 213 (1973);

(b) J. S. Binkley and J. A. Pople, *J. Chem. Phys.* **66**, 879 (1977).

¹²J. Baker (unpublished).

¹³GAUSSIAN 82, J. S. Binkley, M. J. Frisch, D. J. Defrees, K. Raghavachari, R. A. Whiteside, H. B. Schlegel, E. M. Fluder, and J. A. Pople, Carnegie-Mellon University, Pittsburgh, PA.

¹⁴C. Sosa and H. B. Schlegel, *Int. J. Quantum Chem.* **29**, 1001 (1986).

¹⁵P. J. Knowles and N. C. Handy, *Chem. Phys. Lett.* **111**, 315 (1984).